



# Club cells inhibit alveolar epithelial wound repair *via* TRAIL-dependent apoptosis

Khondoker M. Akram\*, Nicola J. Lomas\*<sup>#,</sup>, Monica A. Spiteri\*<sup>†</sup>  
and Nicholas R. Forsyth\*

**ABSTRACT:** Club cells (Clara cells) participate in bronchiolar wound repair and regeneration. Located in the bronchioles, they become activated during alveolar injury in idiopathic pulmonary fibrosis (IPF) and migrate into the affected alveoli, a process called alveolar bronchiolisation. The purpose of this migration and the role of club cells in alveolar wound repair is controversial. This study was undertaken to investigate the role of club cells in alveolar epithelial wound repair and pulmonary fibrosis.

A direct-contact co-culture *in vitro* model was used to evaluate the role of club cells (H441 cell line) on alveolar epithelial cell (A549 cell line) and small airway epithelial cell (SAEC) wound repair. Immunohistochemistry was conducted on lung tissue samples from patients with IPF to replicate the *in vitro* findings *ex vivo*.

Our study demonstrated that club cells induce apoptosis in alveolar epithelial cells and SAECs through a tumour necrosis factor-related apoptosis-inducing ligand (TRAIL)-dependent mechanism resulting in significant inhibition of wound repair. Furthermore, in IPF lungs, TRAIL-expressing club cells were detected within the affected alveolar epithelia in areas of established fibrosis, together with widespread alveolar epithelial cell apoptosis.

From these findings, we hypothesise that the extensive pro-fibrotic remodelling associated with IPF could be driven by TRAIL-expressing club cells inducing apoptosis in alveolar epithelial cells through a TRAIL-dependent mechanism.

**KEYWORDS:** Alveolar bronchiolisation, apoptosis, club cells (Clara cells), idiopathic pulmonary fibrosis

Idiopathic pulmonary fibrosis (IPF) is a chronic progressive fibrosing interstitial pneumonia of unknown aetiology, occurring primarily in older adults and limited to the lungs [1]. The pathophysiological process of this disease is not well understood. However, recently it has been hypothesised that multiple micro-injuries to alveolar epithelial cells, imbalanced immune response and abnormal wound repair are the key mediators of IPF pathogenesis where inflammation may not be an initiating trigger [2–4]. After injury, the restoration of alveolar integrity and functionality through rapid re-epithelialisation of the denuded alveolar basement membrane through alveolar epithelial cell migration, proliferation and differentiation is essential. In IPF this healing process seems to be impaired [2]; while the precise mechanism for this remains uncertain, it is likely to involve multifactorial interactive processes of

repeated injury and substantial type I alveolar epithelial cell loss [2, 5], increased alveolar epithelial cell apoptosis [6–8], dysregulated epithelial–mesenchymal cross-talk [9], polarised immune response [4, 10] and alveolar bronchiolisation [11, 12].

Alveolar bronchiolisation, a process of abnormal proliferation and alveolar migration of club cells (Clara cells) and other bronchiolar epithelial cells, has been documented in both IPF lung tissues and animal models of pulmonary fibrosis [11–18]. A sub-population of these club cells behaves as functional bronchiolar progenitor cells, with participation in bronchiolar wound repair and regeneration [19–21]. However, lineage tracking in animal model studies has indicated that club cells may not take part in alveolar injury repair [22]. Also, in bleomycin-induced murine pulmonary fibrosis, abrogation of alveolar bronchiolisation

## AFFILIATIONS

\*Institute for Science and Technology in Medicine, School of Postgraduate Medicine, Keele University,

<sup>#</sup>Dept of Cellular Pathology, and

<sup>†</sup>Dept of Respiratory Medicine, University Hospital of North Staffordshire, Stoke-on-Trent, UK.

## CORRESPONDENCE

N.R. Forsyth  
Institute for Science and Technology in Medicine

Guy Hilton Research Centre  
School of Postgraduate Medicine  
Keele University  
Stoke-on-Trent  
ST4 7QB  
UK

E-mail: n.r.forsyth@pmed.keele.ac.uk

Received:

Dec 05 2011

Accepted after revision:

June 22 2012

First published online:

July 12 2012

This article has supplementary material available from [www.erj.ersjournals.com](http://www.erj.ersjournals.com)

In accord with the decision of the Committee of Respiratory Journal Editors, the name “club cell” is now recommended and will be used in place of “Clara cell” in the *European Respiratory Journal*.

European Respiratory Journal  
Print ISSN 0903-1936  
Online ISSN 1399-3003

does not worsen the disease state [15]. Despite these findings, alveolar bronchiolisation remains a constant histological feature in IPF lungs accompanied by failed alveolar architecture and functionality restoration [11, 12, 14]. We hypothesise that with the onset of IPF, the activated migration of club cells towards the alveolar regions and their interaction with *in situ* alveolar epithelial cells is pivotal to the consequent aberrant repair response and ensuing fibrotic tissue remodelling. Elucidation of this key club cell–alveolar epithelial cell interaction could unravel exploitable targets for pharmacological manipulation beneficial to IPF, a disease for which there is still no efficacious treatment.

Accordingly, in this study we developed a two-cell co-culture wound repair model to clarify the role of club cells in alveolar epithelial cell wound repair. By using this model we demonstrated that direct contact of club cells significantly inhibited alveolar epithelial cell and small airway epithelial cell (SAEC) wound repair *via* tumour necrosis factor-related apoptosis-inducing ligand (TRAIL)-dependent apoptosis. By expanding this finding in lung tissue samples of patients with IPF, we demonstrated the localisation of TRAIL-expressing club cells in alveolar regions close to the established fibrosis together with *in situ* widespread alveolar epithelial cell apoptosis. These *in vitro* and *ex vivo* findings lead us to hypothesise that extensive profibrotic remodelling during IPF is potentially driven by TRAIL-expressing club cells inducing apoptosis in alveolar epithelial cells through a TRAIL-dependent mechanism.

## MATERIALS AND METHODS

### Human cell lines

Human type II alveolar epithelial cell line A549, club cell line H441, normal human lung fibroblasts CCD-8Lu (all from ATCC, Rockville, MD, USA) and human primary SAECs (Lonza, Wokingham, UK) were cultured according to the manufacturers' protocol. As human primary type II alveolar epithelial cells (ScienceCell Research Laboratory, Carlsbad, CA, USA) do not form confluent monolayers, a primary criterion for wound repair models, we used prosurfactant protein (proSP)-C (a type II alveolar epithelial cell marker)-expressing A549 cells (online supplementary figure E1). Experiments were replicated on the confluent monolayer-capable proSP-C-negative SAECs (online supplementary figure E1) to exclude the potential for cancer cell line-related bias. Due to the unavailability of primary human club cells, the H441 cell line, which originated from human club cells and is widely used in club cell functional studies [23–25], was chosen.

### Human tissue samples

Lung tissue samples were obtained from 21 patients with IPF and 19 control subjects with no evidence of IPF but who had undergone lobectomy for other reasons. IPF tissue diagnosis was confirmed by an independent pathologist following the histopathological criteria described by the American Thoracic Society (ATS) and the European Respiratory Society (ERS) [1].

### *In vitro* epithelial cell wound repair assay

The *in vitro* wound repair assay was a modification of a previously described methodology [26]. Briefly, A549 and H441 cells were cultured to confluence as monolayers using 10% fetal bovine serum (FBS)-supplemented complete Dulbecco's

modified Eagle medium (DMEM) under standard conditions. Linear wounds were made on cell monolayers and then replenished with either serum-free (SF)-DMEM, 10% FBS-supplemented DMEM, or SF-conditioned media (CM) for 24 h (figs 1a and 2a). Circumferential wound gaps were measured by Image J software (National Institutes of Health, Bethesda, MD, USA) and the percentage of wound repair after 24 h was calculated.

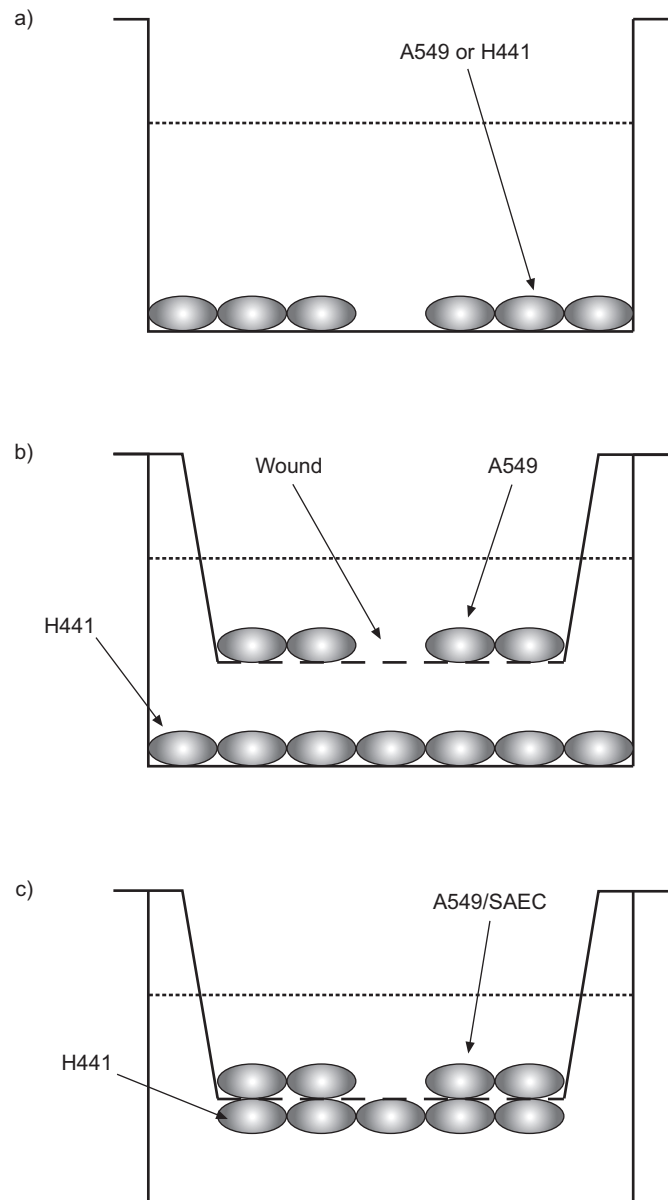


**FIGURE 1.** *In vitro* epithelial wound repair and co-culture system. a) Scratch wound on A549 or H441 cell monolayer on 24-well plate. b) Indirect-contact co-culture model. Wounded A549 on 0.4- $\mu$ m porous polyethylene terephthalate (PET) membrane of transwell (upper layer) with H441 cells (bottom layer); the gap between the two cell layers is 0.8 mm. c) Direct-contact co-culture model. Dil-labelled wounded A549 cells or small airway epithelial cells (SAEC) (upper layer) with un-wounded DiO-labelled H441 cells (bottom layer) grown on 3- $\mu$ m porous transwell PET membranes. After wounding, the direct- and indirect-contact samples were cultured in serum-free basal media for 24 h.

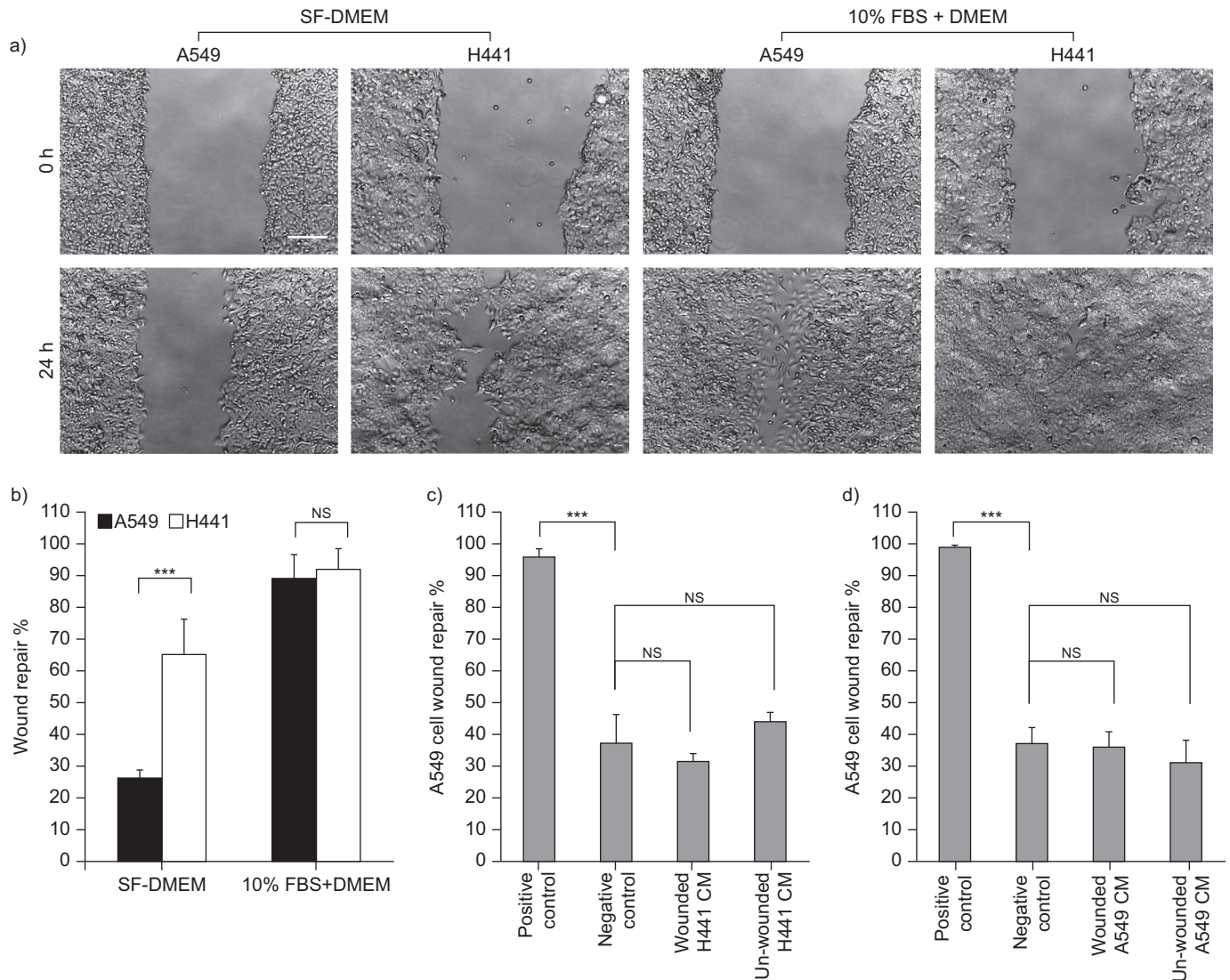


**FIGURE 2.** A549 and H441 cell *in vitro* wound repair. a) A549 and H441 cell wound repair with serum-free (SF)-Dulbecco's modified Eagle medium (DMEM) and 10% fetal bovine serum (FBS)-containing DMEM at 0 h and after 24 h. Scale bars=200  $\mu$ m. b) Wound repair of A549 and H441 cells in SF- and 10% FBS-supplemented media after 24 h (n=4, five or more replicates each). c) A549 wound repair after 24 h with SF-conditioned media (CM) of wounded and un-wounded H441 cells (n=3, four replicates each). d) A549 cell wound repair after 24 h with SF-CM of wounded and un-wounded A549 cell (n=3, three replicates each). Positive and negative controls represent wound repair with 10% FBS-supplemented and SF media, respectively. \*\*\*:  $p < 0.001$ . ns: not significant. Data are presented as mean  $\pm$  sd.

### Direct- and indirect-contact co-culture wound repair assays

For the direct-contact co-culture wound repair experiment, DiI-labelled A549 cells or SAECs and DiO-labelled H441 or CCD-8Lu cells (Vybrant™ Multicolor Cell Labeling Kit; Invitrogen, Paisley, UK) were grown to confluence on the contralateral surfaces of 3- $\mu$ m porous polyethylene terephthalate (PET) transwell membranes (BD Bioscience, Franklin Lakes, NJ, USA) (figs 1c, 3d and e). For indirect-contact co-culture, A549 cells were grown on the upper surface of 0.4- $\mu$ m porous PET transwell membranes and H441 or CCD-8Lu cells on the bottom surface of the well plate (fig. 1b). Linear wounds were made on A549 cell or SAEC monolayers. Wounded A549 cells or SAECs were then cultured in serum-free basal media for 24 h. Prior to imaging of the direct-contact model, H441 or CCD-8Lu cells were removed carefully with a cotton swab from the undersurface of the PET membrane. Images of direct-contact co-culture were acquired with a laser

scanning confocal microscope (Olympus, Southend-on-Sea, UK) at 0 and 24 h. Images of indirect-contact co-culture wounds were taken by an inverted light microscope, as previously described. Wound gap measurement and wound repair analysis were performed as previously described.

For assessment of H441 cell migration in A549–H441 or SAEC–H441 cell direct-contact co-culture, DiO-labelled H441 cells and DiI-labelled A549 cells or SAECs were counted at the respective wound sites at 0 h and after 24 h of wounding (fig. 3d and e). Confocal Z-scanning was performed to confirm the migration.

### Assessment of apoptosis in alveolar A549 cells and SAECs

Ligand-induced apoptosis in wounded A549 cell monolayers was assessed by using recombinant human soluble TRAIL or Fas ligand (FasL) (Peprotech, Rocky Hill, NJ, USA), which was



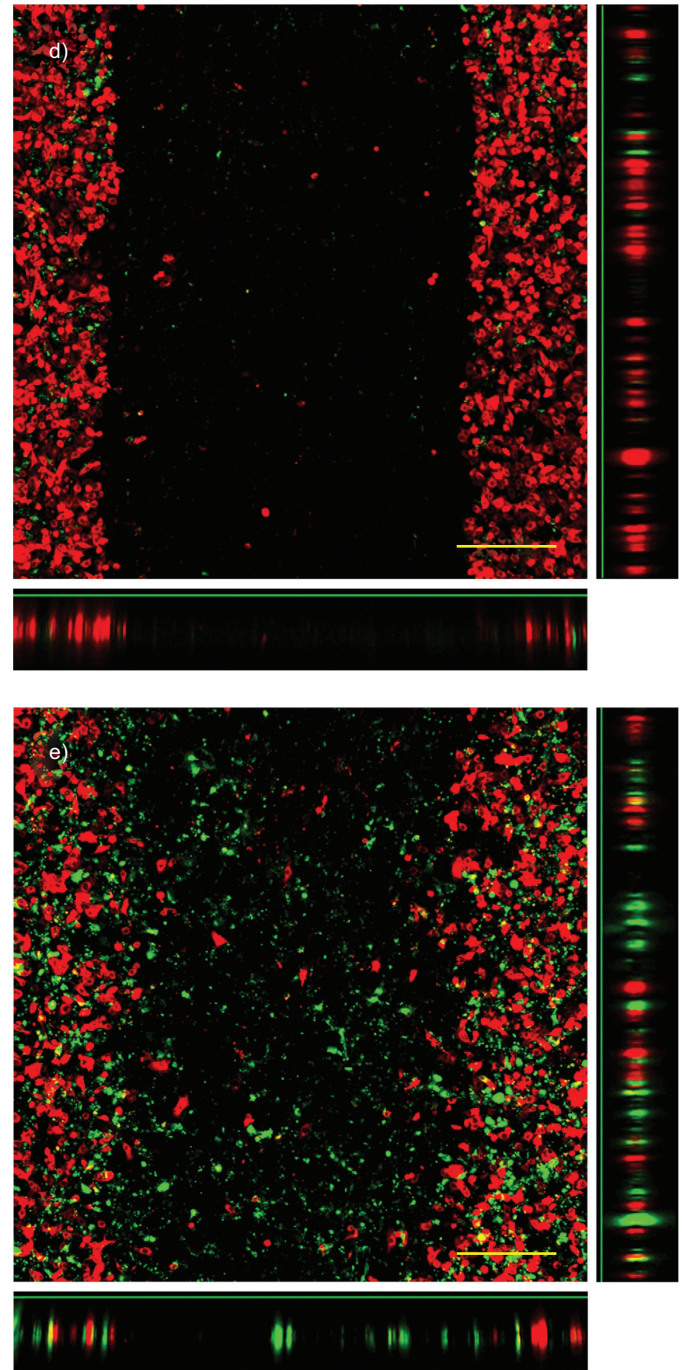
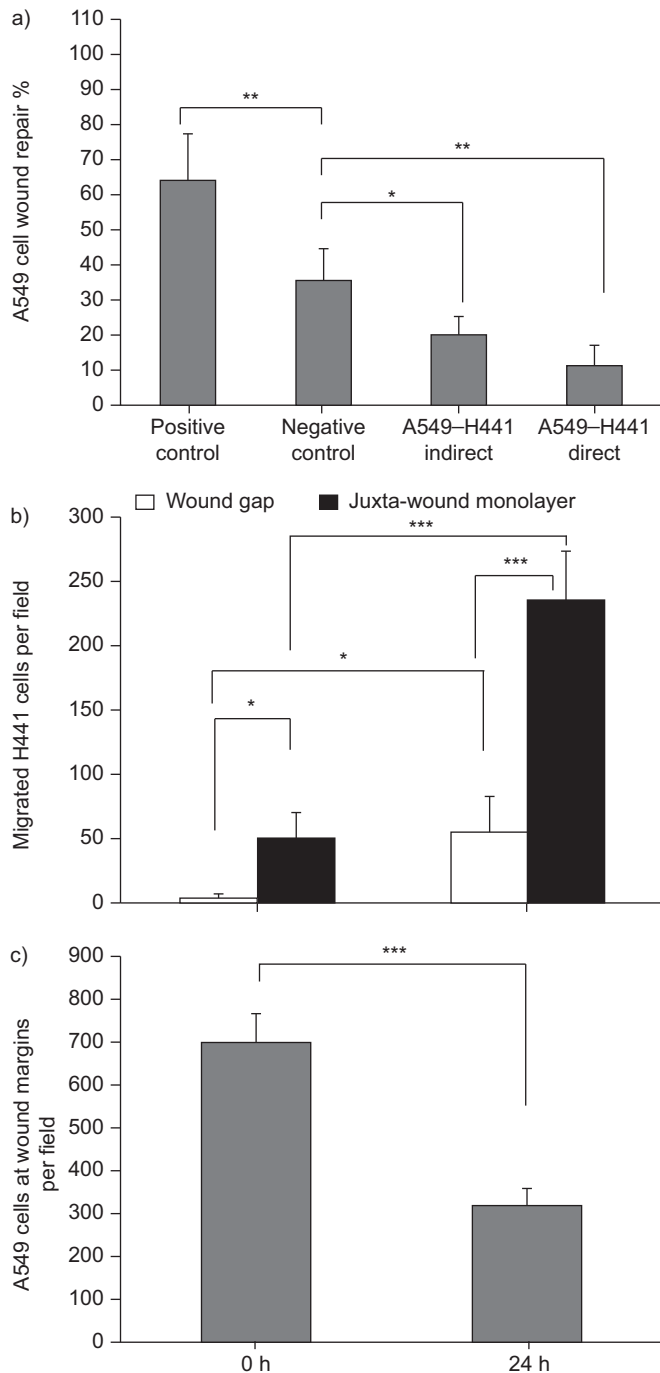


**FIGURE 3.** A549-H441 direct- and indirect-contact co-culture wound repair. a) A549 cell wound repair after 24 h in direct- and indirect-contact co-culture with H441 cells. Positive and negative control represent the wound repair with 10% fetal bovine serum-supplemented and serum-free media, respectively ( $n=4$ , three replicates each). b) Migration of H441 cells into the A549 juxta-wound monolayers and wound gaps ( $n=5$ ). c) Number of A549 cells per field at the juxta-wound monolayers in direct-contact co-culture with H441 cells after 24 h ( $n=5$ ). d, e) Laser scanning confocal microscopic images of A549-H441 direct-contact co-culture at 0 and 24 h, respectively. DiI-labelled red cells are A549 and DiO-labelled green cells are H441. Vertical side bars represent Z-slicing through the corresponding juxta-wound monolayers, whereas horizontal bars represent Z-slicing through wound gaps. A significant proportion of migrated H441 cells were noted at the juxta-wound monolayers of A549 cells after 24 h of wounding (e). \*:  $p<0.05$ ; \*\*:  $p<0.01$ ; \*\*\*:  $p<0.001$ . Data are presented as mean  $\pm$  SD. Scale bars=150  $\mu$ m.

also blocked by their specific receptor-blocking monoclonal antibodies (mAbs) TRAIL-R1 (HS101,  $10 \mu\text{g}\cdot\text{mL}^{-1}$ ) and/or TRAIL-R2 (HS201,  $10 \mu\text{g}\cdot\text{mL}^{-1}$ ), and Fas (SM1/23,  $10 \mu\text{g}\cdot\text{mL}^{-1}$ ) (Enzo Life Science, Lausen, Switzerland). Soluble TRAIL-induced

apoptosis was also assessed in SAECs. To assess H441 or CCD-8Lu cell direct-contact induced apoptosis in A549 cells or SAECs, DiI-labelled A549 cells or SAECs were co-cultured with unlabelled H441 or CCD-8Lu cells in direct-contact wound repair



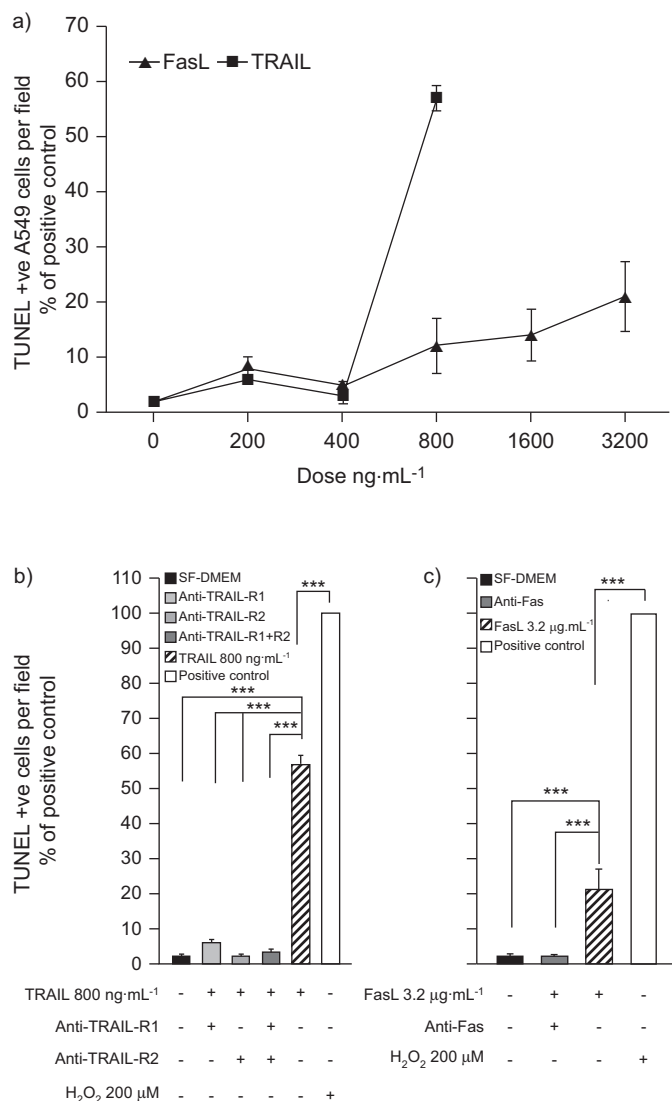


**FIGURE 4.** Assessment of apoptosis in A549 cell monolayers. a) Dose-response of apoptosis induction in A549 cells with soluble Fas ligand (FasL) and tumour necrosis factor-related apoptosis-inducing ligand (TRAIL). b) Blocking of TRAIL-induced apoptosis in A549 by anti-TRAIL-receptor (R)1 or anti-TRAIL-R2 or combined monoclonal antibodies (mAbs). c) Blocking of soluble FasL-induced apoptosis in A549 cells with anti-Fas mAb (n=3). Positive controls represent apoptosis in A549 cells induced by 200 μM H<sub>2</sub>O<sub>2</sub>. Data plots and columns represent mean experiment values ± SD. TUNEL: terminal deoxynucleotidyl transferase-mediated deoxyuridine triphosphate nick-end labelling; SF: serum free; DMEM: Dulbecco's modified Eagle medium; H<sub>2</sub>O<sub>2</sub>: hydrogen peroxide. \*\*\*: p<0.001.

settings, as previously described. To block H441 cell-induced apoptosis, samples were pre-treated with Fas (SM1/23, 10 μg·mL<sup>-1</sup>) or TRAIL-R1/R2 (HS101, HS201; 10 μg·mL<sup>-1</sup>) receptor-blocking antagonistic mAbs. Apoptosis was assessed after 24 h of wounding by the TUNEL (terminal deoxynucleotidyl transferase-mediated deoxyuridine triphosphate nick-end labelling) assay method using an *In Situ* Cell Death Detection Kit, Fluorescein (Roche Diagnostics Limited Applied Science, Burgess Hill, UK). For positive controls, apoptosis was induced in A549 cells or SAECs by 200 μM hydrogen peroxide (H<sub>2</sub>O<sub>2</sub>) and negative controls were treated with SF-basal media.

### Further experimental procedures

Additional detailed experimental procedures are described in the online supplementary material.

### Statistical analysis

The significance of difference between two groups was determined by paired, two-tailed t-tests. Differences between three or more groups were analysed with non-parametric one-way ANOVA, with *post hoc* Tukey's multiple comparison analysis. Patient data were analysed by Wilcoxon matched-pairs signed rank test or Mann-Whitney U-test. A p-value of <0.05 was considered to indicate statistical significance. *In vitro* data are presented as mean ± SD and patient data are presented as mean ± SEM. Statistical analysis was conducted using GraphPad Prism version 5.00 software for Windows (GraphPad Software, San Diego, CA, USA).

### Study approval

Human tissue research was approved by the South Staffordshire Local Research Ethics Committee (08/H1203/6).

## RESULTS

### H441 (club) cells do not stimulate A549 cell wound repair through paracrine factors

To establish cross-talk between secretory products of alveolar and bronchiolar cells we first investigated the wound repair patterns of A549 and H441 cells using an *in vitro* wound repair model (figs 1a and 2a) [26]. The H441 cells are slow-growing in comparison to A549 cells in both SF and 10% serum-supplemented media (online supplementary figure E2a and b). The calculated doubling times of A549 and H441 cells in SF media were 22 and 100 h, respectively, and 18 and 50 h, respectively, in 10% FBS-supplemented media (online supplementary figure E2c). In spite of this difference, in the presence of 10% serum, no significant differences in wound repair patterns were observed (fig. 2a and b). However, in SF media, the rate of H441 cell wound repair was 2.5-fold than that seen for A549 cells (65% H441 *versus* 26% A549, p<0.001; fig. 2b).

Next, we tested SF-CM obtained from wounded and unwounded H441 and A549 cell monolayers on A549 cell wound repair. SF-CM from both wounded and unwounded H441 cells did not affect A549 cell wound repair (32% SF-CM *versus* 38% SF, 44% SF-CM *versus* 38% SF, respectively; fig. 2c). Likewise, SF-CM from alveolar A549 cells, irrespective of wounding, did not stimulate any effects on A549 cell wound repair (fig. 2d). In contrast, SF-CM of wounded and unwounded A549 cells did not stimulate H441 cell wound repair (online supplementary figure E3). Taken together, this indicates that club cells (H441 cells) can auto-stimulate wound repair in SF conditions but cannot stimulate repair of alveolar epithelial cell wounds.

### H441 cells inhibit A549 cell wound repair in a A549-H441 co-culture wound repair system

To further explore the role of H441 cells in alveolar A549 cell wound repair, we developed a direct- and indirect-contact co-culture wound repair system (fig. 1b and c). Direct- and indirect-contact co-culture of H441 with wounded A549 monolayers significantly reduced wound repair rates after 24 h of wounding (direct-contact: 11%, p<0.01; indirect-contact: 20%, p<0.05; control: 36%; fig. 3a).

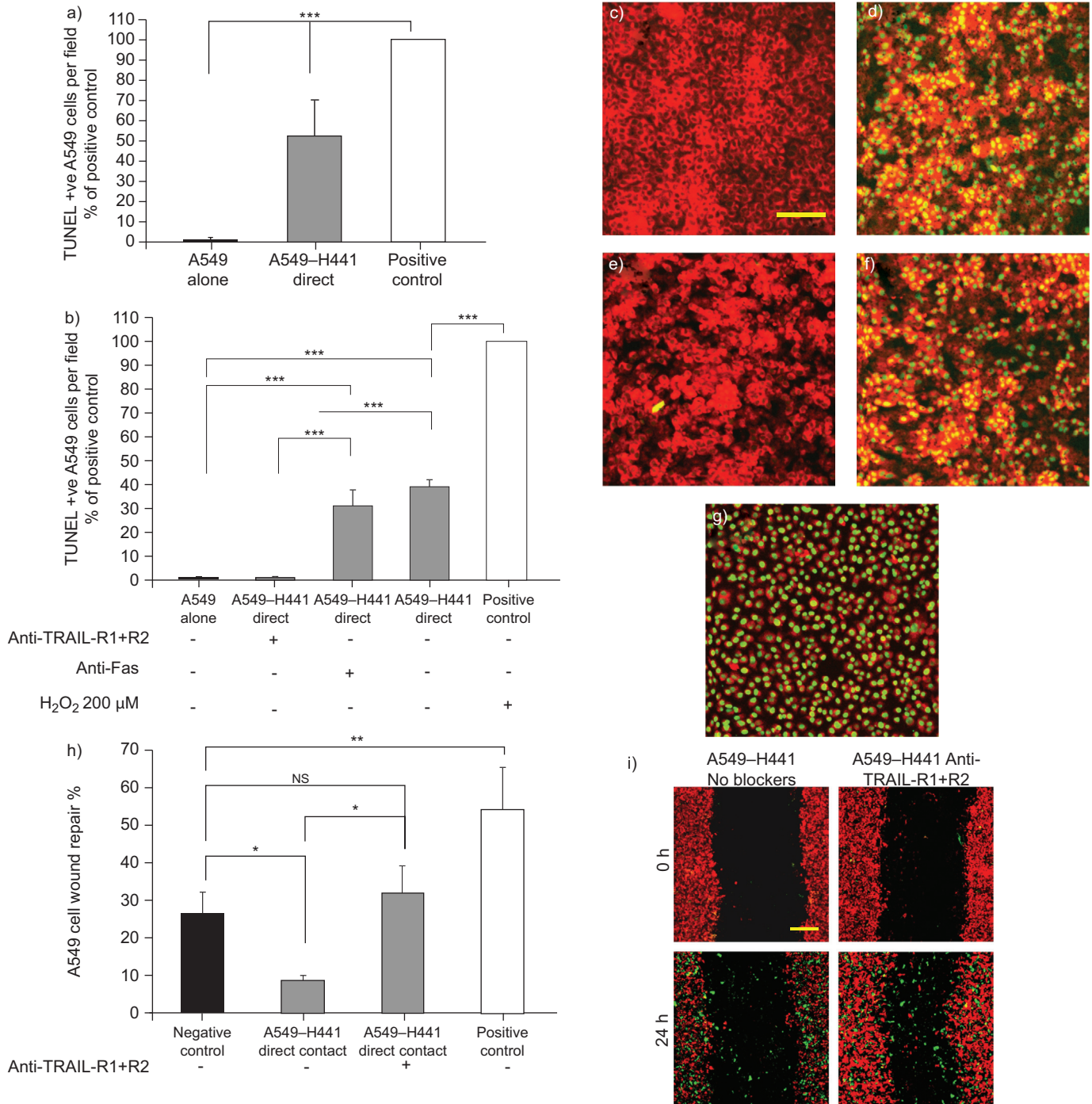


**FIGURE 5.** Assessment of apoptosis and wound repair in A549-H441 direct-contact co-culture. a) Apoptosis in A549 cells at juxta-wound monolayers after 24 h in A549-H441 direct-contact co-culture wound repair (n=3). b) A549-H441 direct-contact co-culture induced apoptosis blocking with anti-tumour necrosis factor-related apoptosis-inducing ligand (TRAIL)-receptor (R)1+R2 and anti-Fas monoclonal antibodies (mAbs). For positive control, apoptosis was induced in A549 cell monolayers by 200 μM H<sub>2</sub>O<sub>2</sub> and for negative control, A549 monolayers were treated with serum-free (SF)-Dulbecco's modified Eagle medium (DMEM) only (n=3). c-g) Laser scanning confocal microscopic images of terminal deoxynucleotidyl transferase-mediated deoxyuridine triphosphate nick-end labelling (TUNEL) assay on A549-H441 direct-contact co-culture. Red cells are Dil-labelled A549 cells and green nuclei are TUNEL-positive A549 cell nuclei. c) A549 cell monoculture (as negative control). d) A549-H441 cell direct-contact co-culture. e) A549-H441 direct-contact co-culture with anti-TRAIL-R1 and -R2 mAbs. f) A549-H441 direct-contact co-culture with anti-Fas mAb. g) Positive control: apoptosis induced in A549 monoculture with 200 μM H<sub>2</sub>O<sub>2</sub>. h) A549 wound repair in presence and absence of anti-TRAIL-R1+R2 mAbs (10 μg·mL<sup>-1</sup>) in A549-H441 direct-contact co-culture after 24 h. Negative and positive control represent A549 cell wound repair on transwell membrane in monoculture with SF- and 10% fetal bovine serum (FBS)-containing DMEM, respectively (n=3). i) Representative laser scanning confocal microscopic images of A549-H441 direct-contact co-culture wound repair. Dil-labelled red cells are A549 and DiO-labelled green cells are migrated H441 cells. Results are presented as mean ± SD. ns: not significant; H<sub>2</sub>O<sub>2</sub>: hydrogen peroxide. \*: p<0.05; \*\*: p<0.01; \*\*\*: p<0.001. Scale bars=100 μm (c, d, e, f and g) and 150 μm (i).

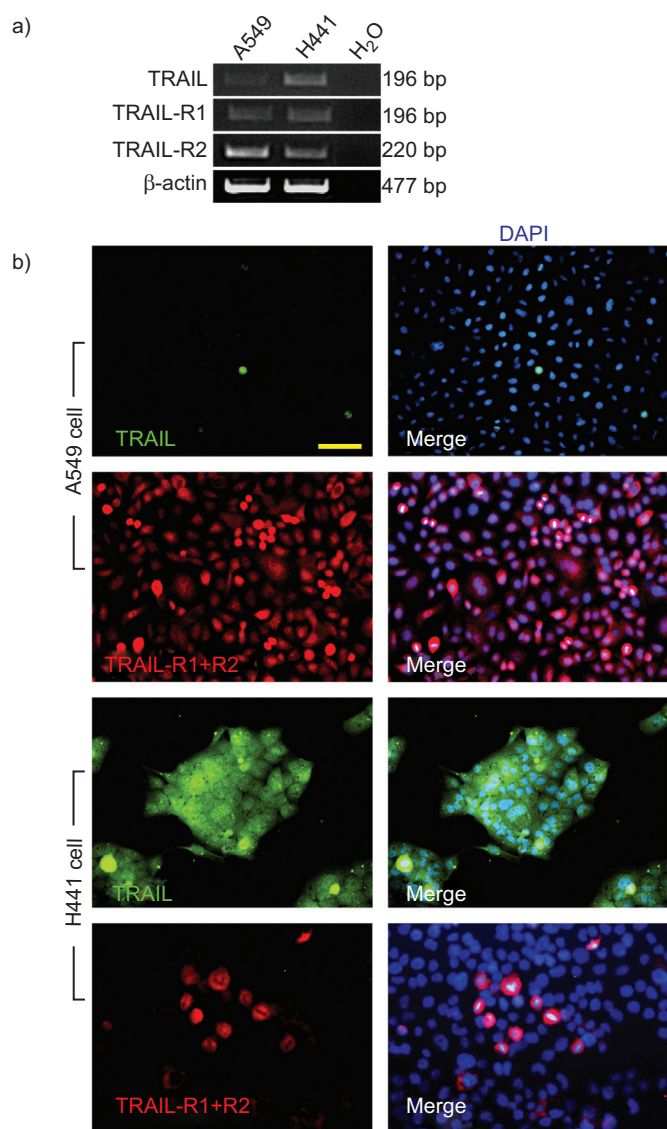


**FIGURE 6.** Tumour necrosis factor-related apoptosis-inducing ligand (TRAIL) and TRAIL receptor (R) expression profile. a) RT-PCR of TRAIL, TRAIL-R1, and TRAIL-R2 of A549 and H441 cells. b) Immunocytochemistry for TRAIL, TRAIL-R1 and TRAIL-R2 in A549 and H441 cells. 4',6-diamidino-2-phenylindole (DAPI) was used for counter-staining of nuclei. Scale bars=50  $\mu\text{m}$ .

Coupled with the reduction in repair rate in A549 cell wounds we also observed substantial H441 cell migration into the wounded A549 cell monolayers where a 4.25-fold greater number of migrated H441 cells were located at the juxta-wound monolayers site in comparison to the wound gap itself ( $p < 0.001$ ; fig. 3b and e). Coupled to this migration, a 55% reduction of A549 cells at the juxta-wound monolayers was also noted (fig. 3c and e). H441 cells did not migrate into the uninjured alveolar epithelial cell monolayer in a similar direct-contact co-culture experiment (online supplementary figure E4), and in the absence of A549 cells, H441 cell migration was negligible (online supplementary figure E5). In contrast, normal human lung fibroblasts CCD-8Lu did not inhibit A549 cell wound repair in A549–CCD-8Lu direct- and indirect-contact co-culture (online supplementary figure E6a). Moreover, CCD-8Lu cell migration to the A549 cell wound site in

the direct-contact model was negligible (online supplementary figure E6b). Taken together, these results suggest that H441 (club) cells, but not normal lung fibroblasts, inhibit alveolar A549 cell wound repair in a proximity-dependent manner where, at least for the direct-contact model, wound repair inhibition was due to direct interruption and destruction of alveolar epithelial cell population.

#### **Soluble TRAIL and FasL induce apoptosis in A549 cells**

We hypothesised that the reduction in A549 cell numbers at juxta-wound sites could be due to H441-induced apoptosis. To test this hypothesis we first examined the sensitivity of A549 cells to established apoptosis-inducing ligands TRAIL and FasL [27–30]. Significant apoptosis was induced in A549 cell monolayers with either soluble TRAIL or FasL at  $800 \text{ ng}\cdot\text{mL}^{-1}$  or  $3.2 \text{ }\mu\text{g}\cdot\text{mL}^{-1}$ , respectively (fig. 4a). The specificity of TRAIL-induced apoptosis was established by A549 cell pre-treatment with anti-TRAIL-receptor (R)1 and/or anti-TRAIL-R2 antagonistic mAbs (fig. 4b). FasL-induced apoptosis specificity was demonstrated *via* the use of the anti-Fas antagonistic mAb (fig. 4c). This indicated the presence of functional Fas and TRAIL receptors on alveolar A549 cells.

#### **Direct contact of H441 cells induces apoptosis in A549 cells in a A549–H441 direct-contact co-culture wound repair system through a TRAIL-dependent mechanism**

To confirm our earlier hypothesis we performed the TUNEL assay on A549 cell wounds in the direct-contact model with H441 cells. We observed a significant rate of apoptosis in A549 cells (52% normalised to positive control) in the juxta-wound margins in the A549–H441 direct-contact wound repair model (fig. 5a and d), which was not observed in the equivalent direct-contact A549–CCD-8Lu co-culture (online supplementary figure E6c). Migratory H441 cells did not stain positively for TUNEL and were therefore not considered to be apoptotic (online supplementary figure E7). Pre-incubation of A549 cells with a blocking antibody specific to Fas, prior to seeding into the direct-contact model with H441 cells, failed to block the apoptotic response (fig. 5b and f). However, pre-incubation of A549 cells with anti-TRAIL R1/R2 mAbs completely blocked H441-induced apoptosis in the direct-contact model ( $p < 0.001$ ; fig. 5b and e) and improved A549 cell wound repair over its untreated counterpart (32% anti-TRAIL-receptor mAbs treated *versus* 8% untreated sample;  $p < 0.05$ ; fig. 5h and i). These results demonstrate that H441 cells induce apoptosis in wounded alveolar A549 cells and inhibit wound repair through a TRAIL-dependent mechanism in a direct-contact co-culture wound repair system.

#### **TRAIL expression profile in H441 and A549 cells**

Transcriptional analysis confirmed TRAIL, TRAIL-R1 and TRAIL-R2 mRNA expression in both un-wounded H441 and A549 (fig. 6a). Immunocytochemistry detected a higher level of TRAIL-R1 and -R2 expression in un-wounded alveolar A549 cells than H441 cells, while the converse was true for TRAIL (fig. 6b).

#### **H441 cells migrate to SAEC wound sites and induce apoptosis in the SAEC–H441 direct-contact co-culture wound repair system**

Although SAECs are proSP-C negative (data not shown) and do not represent type II alveolar epithelial cells, due to their



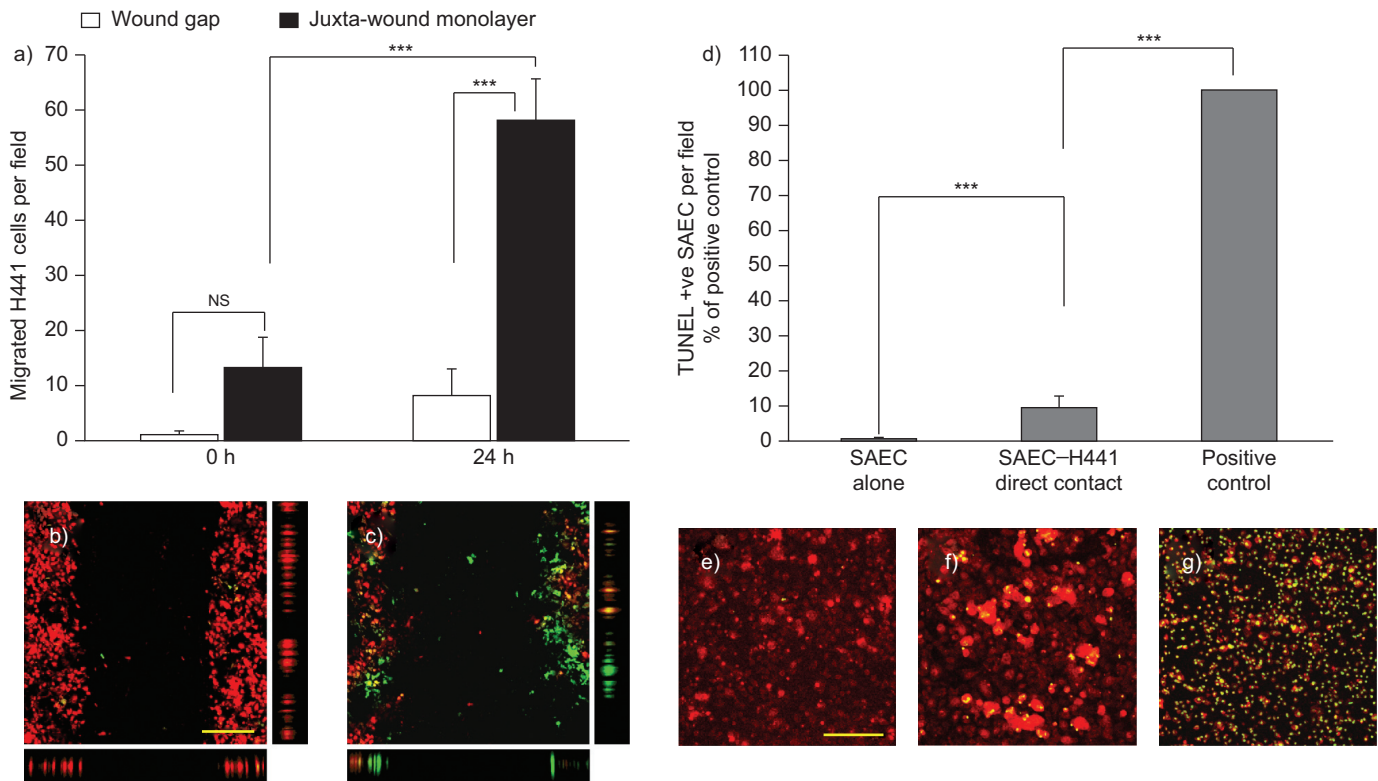


**FIGURE 7.** Small airway epithelial cell (SAEC)-H441 direct-contact co-culture wound repair. a) Migration of H441 cells into the SAEC juxta-wound monolayers and wound gaps ( $n=3$ ). b, c) Laser scanning confocal microscopic images of SAEC-H441 direct-contact co-culture at b) 0 h and c) 24 h. DiI-labelled red cells are SAECs and DiO-labelled green cells are H441 cells. Vertical side bars indicate Z-slicing through the corresponding juxta-wound monolayers and horizontal bars indicate Z-slicing through the wound gap. d) Apoptosis in SAECs at juxta-wound monolayers after 24 h in SAEC-H441 direct-contact co-culture wound repair ( $n=3$ ). For positive control, apoptosis was induced in SAEC monolayers by treatment of 200  $\mu\text{M}$  of hydrogen peroxide ( $\text{H}_2\text{O}_2$ ) for 24 h and for negative control, SAEC monolayers were treated with serum-free small airway basal media only. e-g) Laser scanning confocal microscopic images of terminal deoxynucleotidyl transferase-mediated deoxyuridine triphosphate nick-end labelling (TUNEL) assay on SAEC-H441 direct-contact co-culture. Red cells are DiI-labelled SAECs and green nuclei are TUNEL-positive SAEC nuclei. e) Negative control, SAEC monoculture. f) SAEC-H441 cell direct-contact co-culture wound repair. g) Positive control. Results are presented as mean  $\pm$  SD. NS: not significant. \*\*\*:  $p<0.001$ . Scale bars=200  $\mu\text{m}$ .

suitability for the wound repair model [31] and biological relevance to our experiments we replicated a set of major experiments that were conducted using A549 cells to exclude the potential of cancer cell line-related bias in our results. First, we assessed the migratory properties of H441 cells towards wounded SAEC monolayers. Interestingly, our experiments recapitulated the observations noted in the A549-H441 direct-contact co-culture model. A significant proportion of H441 cells migrated to the SAEC wound sites after 24 h of wounding where a 7.25-fold greater number of migrated H441 cells were located at the juxta-wound monolayers in comparison to the wound gap (58 cells per field *versus* eight cells per field,  $p<0.001$ ; fig. 7a, b and c). The TRAIL-ligand induced an apoptotic response in SAEC which, though reduced in comparison to A549 cells, was demonstrably significant as compared to the relevant control (online supplementary figure E8). Similarly, TRAIL-expressing H441 cells induced significant apoptosis in wounded SAECs in SAEC-H441 direct-contact co-culture when compared to SAEC monoculture (9.54% *versus* 0.38%,  $p<0.001$ ; fig. 7d-f). SAEC were TRAIL-negative (online supplementary figure E9) and confocal microscopy confirmed that TUNEL-positive nuclei were SAECs and not migrated H441 cells (online supplementary

figure E10). In the absence of wounding, negligible numbers of H441 cells migrated towards SAEC layers (data not shown).

#### **TRAIL-expressing club cells are detected in the fibrotic alveoli of IPF lungs with association of alveolar epithelial cell apoptosis**

Histologically, all the IPF biopsy samples showed features in keeping with usual interstitial pneumonia; specifically, a pathognomonic patchwork of normal unaffected lung alternating with remodelled fibrotic lung involving type I pneumocyte destruction, type II pneumocyte hyperplasia in the presence of fibroblastic foci and collagen type scarring. The fibroblastic foci are recognised to reflect sites of active ongoing fibrogenesis.

Localisation of TRAIL-expressing club cells in the alveolar regions of control and IPF lung tissues was investigated by dual immunohistochemistry with the club cell marker (CC)10 and TRAIL antibodies. Dual-labelled CC10/TRAIL club cells were not detected in the alveolar regions of control lungs (fig. 8a) but were observed in the bronchiolar walls (fig. 8b). However, in 18 out of 21 IPF cases studied, CC10/TRAIL-positive club cells were readily detected within the hyperplastic alveolar epithelial

regions (fig. 8d) and in the alveolar epithelium directly overlying fibroblastic foci (fig. 8e). Quantitative analysis displayed an average of 15% CC10/TRAIL-positive epithelial cells across the IPF cases ( $p=0.0004$ ; fig. 8i).

Dual proSP-C/TUNEL labelling was next performed to identify the presence and localisation of apoptotic alveolar epithelial cells in IPF lungs and compared to control tissues (fig. 8f–h). Increased numbers of TUNEL-labelled proSP-C-positive alveolar epithelial cells were detected in the regions of fibroblastic foci and remodelled fibrotic areas in IPF lungs (an average of 37% of proSP-C/TUNEL cells in IPF cases *versus* 11% in controls;  $p=0.0035$ ; fig. 8j). Significantly, 10 out of the examined 12 control cases did not demonstrate TUNEL-labelled alveolar epithelial cells; however, two cases displayed a high number of TUNEL-positive proSP-C-labelled cells for no obvious histological reason, as the control tissue examined was morphologically healthy (fig. 8j). Notwithstanding this finding, taken together the data provide evidence for a potential association of alveolar epithelial cell apoptosis and TRAIL-expressing club cells with an involvement in the propagation of fibrogenesis in pulmonary fibrosis.

## DISCUSSION

The precise role of club cells in the repair of alveolar epithelial injury in IPF remains unknown. A reparative role is unlikely due to failed restoration of normal architecture and lung function after apparent proliferation and migration into injured alveoli in IPF [11, 12]. In this study, we have clarified a likely role of club cells in alveolar epithelial cell wound repair by using an *in vitro* wound repair model and implicated the club cells in the profibrogenic process. This first demonstration that club cells induce apoptosis in alveolar epithelial cell through a TRAIL-dependent mechanism provides evidence of previously undiscovered cell behaviour with implications for lung pathophysiology. We further demonstrated that TRAIL-expressing club cells not only induced apoptosis in an alveolar epithelial cell line but also in primary human SAECs. Club cell behaviours on alveolar epithelial cells were cell-type specific as demonstrated *via* the contrasting behaviour of normal lung fibroblasts on alveolar epithelial cells. In addition, the observation that alveolar bronchiolised club cells express TRAIL and are associated with alveolar epithelial cell apoptosis in IPF lungs suggests that club cells may drive the aberrant alveolar wound repair event cascade and propagate the ensuing fibrogenesis through TRAIL-mediated apoptosis induction in alveolar epithelial cells. Separate in-house studies have demonstrated a significant upregulation of TRAIL-R1 and -R2 receptors in alveolar epithelial cells of IPF lungs, further supporting a potential involvement of TRAIL-mediated apoptosis in alveolar epithelial cells in IPF.

IPF is characterised as a consequence of aberrant alveolar wound repair potentially due to apoptosis, dysregulated epithelial-mesenchymal homeostasis, basement membrane disruption, imbalanced immune response, alveolar epithelial cell loss and alveolar bronchiolisation [2, 4–12]. The role of alveolar bronchiolisation in aberrant wound repair and the precise nature of the interaction between the club cells and alveolar epithelial cells are both relatively undefined. Bronchiolisation has been postulated as an indicator of aberrant alveolar wound repair in chemically induced pulmonary fibrosis and human IPF lung tissue [11, 12].

During fibrogenesis in IPF, club and other bronchiolar cells appear in the alveolar regions of established fibrotic areas and directly contact alveolar epithelial cells. While the precise mechanism is unknown, animal models and *ex vivo* studies on IPF tissue suggest that downregulation of caveolin-1 (a membrane protein that suppresses epithelial proliferation) stimulates bronchiolar and club cell proliferation [11] and upregulation of matrix metalloproteinase-9 facilitates their migration into the affected alveoli, resulting in alveolar bronchiolisation [15]. A recent study has suggested involvement of neuregulin1 $\alpha$ -dependent ectopic mucus cell differentiation in the process of bronchiolisation and lung remodelling in IPF lungs [32]. The migratory aspect of club cell behaviour was confirmed in our model where H441 cells migrated to wounded alveolar A549 cell and SAEC layers, most probably driven by a chemotactic mechanism, as, in the absence of A549 or SAECs, club cell migration was not observed. This migration was accompanied by an inhibitory effect on alveolar epithelial cell wound repair *via* TRAIL-mediated apoptosis of alveolar epithelial cell. TRAIL, a member of the tumour necrosis factor superfamily, can induce apoptosis through interaction with the TRAIL-R1 and TRAIL-R2 receptors (alternatively known as DR4 and DR5, respectively) [27–29]. Although expression of TRAIL and its receptors is detected in many steady-state human cell types [33], their physiological function is poorly understood. However, TRAIL has been shown to play an important role in T-cell-mediated immunomodulatory function and intestinal epithelium homeostasis [34, 35]. Here, the observation that club cells can induce apoptosis in alveolar A549 cells provides support for our hypothesis of the involvement of TRAIL-expressing club cell in the aberrant alveolar wound repair found in IPF.

Pathologically, IPF is characterised by its regional and temporal heterogeneity. Affected alveolar regions in proximity to the fibroblastic foci and collagen deposition displayed increased numbers of TRAIL-expressing club cells (as compared with control healthy lung biopsies) and were associated with elevated alveolar epithelial cell apoptosis. Furthermore, in IPF lungs, TRAIL-positive alveolar epithelial cells were notably present in areas of hyperplastic cuboidalised alveoli and in epithelia overlying fibroblastic foci. In contrast, alveolar epithelial cells of control lungs did not express TRAIL. TRAIL-mediated apoptosis has been reported in other chronic disease states. For instance, in chronic pancreatitis the pancreatic stellate cells overexpress TRAIL and directly contribute to the acinar regression through induction of apoptosis in parenchymal cells *via* a TRAIL-receptor-mediated apoptosis mechanism [36]. TRAIL-mediated apoptosis has been reported as a key mediator for progression of human diabetic nephropathy where TRAIL-overexpression in renal tubular epithelial cells is associated with severe tubular atrophy and interstitial fibrosis [37]. Other studies have demonstrated upregulation of TRAIL in intestinal epithelial cells associated with epithelial cell destruction through TRAIL-mediated apoptosis and progression of inflammatory bowel disease such as ulcerative colitis and Crohn's disease, while downregulation is associated with the refractory stages of the disease [38, 39]. Chronic endoplasmic reticulum stress and Fas-FasL-mediated apoptosis in alveolar epithelial cells and their association in aberrant alveolar wound repair in IPF have







**FIGURE 8.** (Continued from previous page.) f) Pro-surfactant protein (SP)-C/TUNEL dual staining of control lung. TUNEL-positive nuclei were not detected in proSP-C-positive type II alveolar epithelial cells (red fluorophore-labelled). g) proSP-C/TUNEL dual-labelled cells (arrow) were detected in the hyperplastic regions of IPF lung tissue. A heterogeneous pattern of TUNEL-positive alveolar epithelial cells was observed. The arrowhead indicates a proSP-C-only cell. Notable numbers of inflammatory cells in the interstitial spaces were also TUNEL-positive. h) Apoptosis was detected in alveolar epithelial cells overlying the fibroblastic foci in IPF lung (arrow). Magnification:  $\times 200$  for all images. i) Quantitative analysis of CC10/TRAIL dual-positive cells in the alveolar region of normal and IPF lungs (21 IPF patients and 19 controls). j) Quantification of proSP-C/TUNEL-positive cells in the alveolar regions of IPF and healthy control lungs (12 IPF and 12 controls). Data are presented as mean  $\pm$  SEM. #:  $p=0.0004$  (Wilcoxon matched-pairs signed rank test); \*:  $p=0.0035$  (Mann-Whitney U-test).

been reported previously [7, 40]. Combining the literature evidence with our study findings, here we suggest that TRAIL-mediated apoptosis could play a crucial role in alveolar epithelial cell apoptosis and fibrogenesis propagation in IPF; this is probably mediated *via* activated TRAIL-expressing club cells consequent on alveolar bronchiolisation. These findings unravel critical targets for further investigation towards development of novel therapeutic agents, perhaps in combination with tissue-engineered wound repair modelling.

### SUPPORT STATEMENT

This study was supported by a joint award through the Medical Research Council Dorothy Hodgkin Postgraduate Award and the Directorate of Respiratory Medicine Chest Fund, University Hospital of North Staffordshire (Stoke-on-Trent, UK).

### STATEMENT OF INTEREST

None declared.

### REFERENCES

- Raghu G, Collard HR, Egan JJ, *et al.* ATS/ERS/JRS/ALAT statement: idiopathic pulmonary fibrosis: evidence-based guidelines for diagnosis and management. *Am J Respir Crit Care Med* 2011; 183: 788–824.
- Selman M, King TE Jr, Pardo A. Idiopathic pulmonary fibrosis: prevailing and evolving hypotheses about its pathogenesis and implications for therapy. *Ann Intern Med* 2001; 134: 136–151.
- Kaminski N, Belperio JA, Bitterman PB, *et al.* Idiopathic pulmonary fibrosis. *Am J Respir Cell Mol Biol* 2003; 29: S1–S105.
- Strieter RM. Pathogenesis and natural history of usual interstitial pneumonia. The whole story or the last chapter of a long novel. *Chest* 2005; 128: 526S–532S.
- Corrin B, Dewar A, Rodriguez-Roisin R, *et al.* Fine structural changes in cryptogenic alveolitis and asbestosis. *J Pathol* 1985; 147: 107–119.
- Uhal BD, Joshi I, Hughes WF, *et al.* Alveolar epithelial cell death adjacent to underlying myofibroblasts in advanced fibrotic human lung. *Am J Physiol Lung Cell Mol Physiol* 1998; 275: 1192–1199.
- Kuwano K, Miyazaki H, Hagimoto N, *et al.* The involvement of Fas–Fas ligand pathway in fibrosing lung diseases. *Am J Respir Cell Mol Biol* 1999; 20: 53–60.
- Barbas-Filho JV, Ferreira MA, Sesso A, *et al.* Evidence of type II pneumocyte apoptosis in the pathogenesis of idiopathic pulmonary fibrosis (IPF)/usual interstitial pneumonia (UIP). *J Clin Pathol* 2001; 54: 132–138.
- Selman M, Pardo A. Idiopathic pulmonary fibrosis: an epithelial/fibroblastic cross-talk disorder. *Respir Res* 2002; 3: 3.
- Tzouveleakis A, Bouros E, Bouros D. The immunology of pulmonary fibrosis: the role of Th1/Th2/Th17/Treg cells. *Pneumon* 2010; 23: 17–20.
- Odajima N, Betsuyaku T, Nasuhara Y, *et al.* Loss of caveolin-1 in bronchiolisation in lung fibrosis. *J Histochem Cytochem* 2007; 55: 899–909.
- Chilosi M, Poletti V, Murer B, *et al.* Abnormal re-epithelialization and lung remodeling in idiopathic pulmonary fibrosis: the role of  $\Delta N$ -p63. *Lab Invest* 2002; 82: 1335–1345.
- Kawanami O, Ferrans VJ, Crystal RG. Structure of alveolar epithelial cells in patients with fibrotic lung disorders. *Lab Invest* 1982; 46: 39–53.
- Mori M, Morishita H, Nakamura H, *et al.* Hepatoma derived growth factor is involved in lung remodeling by stimulating epithelial growth. *Am J Respir Cell Mol Biol* 2004; 30: 459–469.
- Betsuyaku T, Fukuda Y, Parks WC, *et al.* Gelatinase B is required for alveolar bronchiolisation after intratracheal bleomycin. *Am J Pathol* 2000; 157: 525–535.
- Kawamoto M, Fukuda Y. Cell proliferation during the process of bleomycin-induced pulmonary fibrosis in rats. *Acta Pathol Jpn* 1990; 40: 227–238.
- Fukuda Y, Takemura T, Ferrans VJ. Evolution of metaplastic squamous cells of alveolar walls in pulmonary fibrosis produced by paraquat: an ultrastructural and immunohistochemical study. *Virchows Archiv B Cell Pathol* 1989; 58: 27–43.
- Collins JF, Orozco CR, McCullough B, *et al.* Pulmonary fibrosis with small-airway disease: a model in nonhuman primates. *Exp Lung Res* 1982; 3: 91–108.
- Blundell R. The biology of Clara cells – review paper. *Intl J Mol Med Adv Sci* 2006; 2: 307–311.
- Evans MJ, Johnson LV, Stephens RJ, *et al.* Renewal of the terminal bronchiolar epithelium in the rat following exposure to  $\text{NO}_2$  or  $\text{O}_3$ . *Lab Invest* 1976; 35: 246–257.
- Reynolds SD, Malkinson AM. Clara cell: progenitor for the bronchiolar epithelium. *Intl J Bioch Cell Biol* 2010; 42: 1–4.
- Rawlins EL, Okubo T, Xue Y, *et al.* The role of  $\text{Scgb1a1}^+$  Clara cells in the long-term maintenance and repair of lung airway, but not alveolar, epithelium. *Cell Stem Cell* 2009; 4: 525–534.
- Gazdar AF, Linnoila RI, Kurita Y, *et al.* Peripheral airway cell differentiation in human lung cancer cell lines. *Cancer Res* 1990; 50: 5481–5487.
- Kulaksiz H, Schmid A, Honscheid M, *et al.* Clara cell impact in air-side activation of CFTR in small pulmonary airways. *Proc Natl Acad Sci USA* 2002; 99: 6796–6801.
- Wong PS, Vogel CF, Kokosinski K, *et al.* Arylhydrocarbon receptor activation in NCI-H441 cells and C57BL/6 mice. *Am J Respir Cell Mol Biol* 2010; 42: 210–217.
- Geiser T, Jarreau PH, Atabai K, *et al.* Interleukin-1 $\beta$  augments *in vitro* alveolar epithelial repair. *Am J Physiol Lung Cell Mol Physiol* 2000; 279: L1184–L1190.
- Pan G, O'Rourke K, Chinnaiyan AM, *et al.* The receptor for the cytotoxic ligand TRAIL. *Science* 1997; 276: 111–113.
- Walczak H, Degli-Esposti MA, Johnson RS, *et al.* TRAIL-R2: a novel apoptosis-mediating receptor for TRAIL. *Embo J* 1997; 16: 5386–5397.
- Sheridan JP, Marsters SA, Pitti RM, *et al.* Control of TRAIL-induced apoptosis by a family of signaling and decoy receptors. *Science* 1997; 277: 818–821.
- Griffith ST, Brunner T, Fletcher MS, *et al.* Fas ligand-induced apoptosis as a mechanism of immune privilege. *Science* 1995; 270: 1189–1192.
- O'Toole D, Hassett P, Contreras M, *et al.* Hypercapnic acidosis attenuates pulmonary epithelial wound repair by an NF- $\kappa$ B dependent mechanism. *Thorax* 2009; 64: 976–982.

- 32** Plantier L, Crestani B, Wert SE, *et al.* Ectopic respiratory epithelial cell differentiation in bronchiolised distal airspaces in idiopathic pulmonary fibrosis. *Thorax* 2011; 66: 651–657.
- 33** Daniels RA, Turley H, Kimberley FC, *et al.* Expression of TRAIL and TRAIL receptors in normal and malignant tissues. *Cell Res* 2005; 15: 430–438.
- 34** Falschlehner C, Schaefer U, Walczak H. Following TRAIL's path in the immune system. *Immunology* 2009; 127: 145–154.
- 35** Rimondi E, Secchiero P, Quaroni A, *et al.* Involvement of TRAIL/TRAIL-receptors in human intestinal cell differentiation. *J Cell Physiol* 2006; 206: 647–654.
- 36** Hasel C, Dürr S, Rau B, *et al.* In chronic pancreatitis, widespread emergence of TRAIL receptors in epithelia coincides with neoexpression of TRAIL by pancreatic stellate cells of early fibrotic areas. *Lab Invest* 2003; 83: 825–836.
- 37** Lorz C, Benito-Martin A, Boucherot A, *et al.* The death ligand TRAIL in diabetic nephropathy. *J Am Soc Nephrol* 2008; 19: 904–914.
- 38** Begue B, Wajant H, Bambou J-C, *et al.* Implication of TNF-related apoptosis-inducing ligand in inflammatory intestinal epithelial lesions. *Gastroenterology* 2006; 130: 1962–1974.
- 39** Brost S, Koschny R, Sykora J, *et al.* Differential expression of the TRAIL/TRAIL receptor system in patients with inflammatory bowel disease. *Pathol Res Pract* 2010; 206: 43–50.
- 40** Korfei M, Ruppert C, Mahavadi P, *et al.* Epithelial endoplasmic reticulum stress and apoptosis in sporadic idiopathic pulmonary fibrosis. *Am J Respir Crit Care Med* 2008; 178: 838–846.